Atomically Smooth Stress-Corrosion Cleavage of a Hydrogen-Implanted Crystal

Gianpietro Moras,[1,2,3,*] Lucio Colombi Ciacchi,[4,5] Christian Elsässer,[1,2] Peter Gumbsch,[1,2] and Alessandro De Vita[6,3]

[1]*Karlsruhe Institute of Technology, IZBS—Institute for Reliability of Components and Systems, D-76131 Karlsruhe, Germany*
[2]*Fraunhofer Institute for Mechanics of Materials, D-79108 Freiburg, Germany*
[3]*DEMOCRITOS and CENMAT, I-34127 Trieste, Italy*
[4]*Faculty of Engineering and BCCMS, University of Bremen, D-28359 Bremen, Germany*
[5]*Fraunhofer Institute for Manufacturing Technology and Applied Materials Research, D-28359 Bremen, Germany*
[6]*King's College London, Physics Department, WC2R 2LS London, United Kingdom*

(Received 12 February 2010; published 13 August 2010)

We present a quantum-accurate multiscale study of how hydrogen-filled discoidal "platelet" defects grow inside a silicon crystal. Dynamical simulations of a 10-nm-diameter platelet reveal that H_2 molecules form at its internal surfaces, diffuse, and dissociate at its perimeter, where they both induce and stabilize the breaking up of highly stressed silicon bonds. A buildup of H_2 internal pressure is neither needed for nor allowed by this stress-corrosion growth mechanism, at odds with previous models. Slow platelet growth up to micrometric sizes is predicted as a consequence, making atomically smooth crystal cleavage possible in implantation experiments.

DOI: 10.1103/PhysRevLett.105.075502 PACS numbers: 81.40.Np, 02.70.Ns, 61.72.−y, 85.40.Ry

Stress-corrosion cracking is a multiscale chemo-mechanical phenomenon which poses very significant challenges to atomistic simulation techniques. Its modeling involves dealing with chemical reactions localized at preexisting flaws which both cause and depend on the evolution of the stress field in the whole system [1]. While atomistic models in the size range of 10^4–10^5 atoms are necessary for this class of problems, the direct use of uniformly quantum-accurate models is computationally too demanding. For this reason, despite the very large relevance of stress-corrosion phenomena in materials physics and technology, no quantum-accurate dynamical study of mechanically driven chemical reactions occurring in an extended defect embedded in a brittle matrix has been presented to date.

Here we use a multiscale approach based on a dynamical "quantum-classical (QM/MM) embedding" technique [2] to model the growth of about 10-nm-wide, 1-nm-thick disk-shaped defects which form after targeting high purity crystalline silicon samples with high doses of hydrogen [3,4]. Experimentally, annealing at 400–500 °C determines the growth of these hydrogen-induced platelets (HIPs) [5,6] yielding the formation of micron-sized cracks roughly parallel to the surface [3,7]. This process can be used to slice brittle crystal samples into thin layers bonded to suitable substrates [8], e.g., to produce silicon-on-insulator devices from (100) Si wafers [9]. While a thorough understanding of the complex mechanism of HIP growth would be highly desirable to control the crystal cleavage process with atomic-scale precision, this mechanism remains a matter of speculation [3,4,10]. So far, HIP growth has been modeled by using continuum mechanics and has been assumed to proceed through supercritical crack propagation induced by the internal pressure exerted by H_2 molecules filling the HIPs [11–14]. However, this assumption is not consistent with the experimental production of nanometer-smooth (100) cleavage surfaces [8,15], since (111) and (110) would be the natural cleavage planes of pure Si [16,17].

To solve this apparent contradiction, in this work we simulate the thermal evolution of a realistically sized (100) HIP. To this aim we extend the "learn-on-the-fly" (LOTF) hybrid quantum/classical molecular dynamics (MD) scheme [2], which is specifically suited to investigate extended defects in brittle materials [18], to tackle heterogeneous, nonelemental systems [19]. In our implementation, a mobile and chemically active QM region, described by the density functional tight binding Hamiltonian [20], is seamlessly embedded into a larger system described by the Stillinger-Weber interatomic potential [21]. Consistent with experimental [4,5,22,23] and previous theoretical [24,25] studies, our platelet models are composed of two facing 10-nm-wide dihydride-terminated internal (100) Si surfaces obtained by either replacing an array of Si-Si bonds with Si-H/H-Si bonds [7,25,26] or substituting Si atoms from a (100) layer with terminating H atoms [24,27,28]. Each platelet is embedded in a bulk silicon matrix, leading to model system sizes of up to 35 000 atoms [Figs. 1(a) and 1(b)].

After LOTF geometry optimization (details of the methods are reported in Refs. [19,29]), irrespective of platelet orientation and structure, the relaxed platelet surfaces repel each other. Calculating the atom-resolved stress tensor as in Ref. [30] yields moderate compressive residual stress components along the [010] y axis in the central region above and below the HIP [Fig. 1(c)]. Regions of highly intensified *tensile* stress occur in the vicinity of the platelet edges, with maximum σ_{yy} values up to 16–18 GPa [Fig. 1(d)]. Interestingly, we obtain practically identical stress intensities and distributions for platelet diameters

 © 2010 The American Physical Society

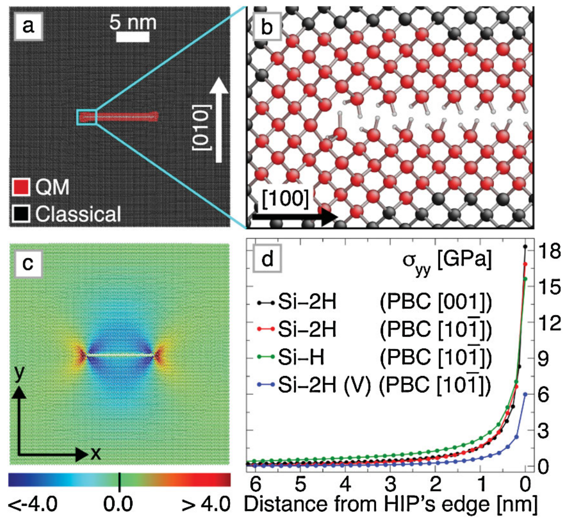

FIG. 1 (color). (a) Atomistic model of a (100) HIP at the center of a 35×35 nm^2 bulk Si model system. One Si cubic primitive cell is repeated along the periodic boundary condition (PBC) z direction (either [001] or [10$\bar{1}$]). The surfaces perpendicular to x and y are instead unconstrained. The LOTF QM region comprises the Si atoms depicted in red and all H atoms. (b) Enlarged picture of a HIP's left edge. (c) Distribution of the σ_{yy} component of the atom-resolved stress tensor for the relaxed HIP system. The color palette ranges from red (tension) to blue (compression) and is limited to the stress value interval -4.0 GPa $\leq \sigma_{yy} \leq 4.0$ GPa. (d) Cross sections of σ_{yy} near the HIP edge for different platelet configurations and orientations. Si-2H and Si-H refer to the dihydride and monohydride HIP surfaces, respectively. V indicates the HIP model obtained by coalescence of hydrogenated vacancies.

ranging from 2 to 10 nm [29]. This suggests that the strength of the stress field in front of the HIP edge is completely determined by the repulsion between the platelet surfaces in a limited region close to its edge, if no external pressure source is present.

Our calculated 3.5% strain of the relaxed edge Si-Si bonds is considerably lower than the typical Si-Si bond critical strain for fracture (~25% [17]). However, it may still be sufficient to promote occasional temporary bond breaking during high-temperature annealing. To address this issue, we carry out several MD simulations at the typical experimental annealing temperature of 800 K. No relevant process occurs in regions of the platelet surface where all Si dangling bonds are fully H-terminated. However, we consistently observe that the presence of one or more unsaturated dangling Si bonds triggers a dihydride-to-monohydride reconstruction of the internal surfaces, accompanied by the formation of H_2 molecules inside the HIP, as hypothesized in Refs. [15,31] (Fig. 2). Crucially, the reaction leaves behind a novel unsaturated Si-H group ready to start yet another "reconstruction/H_2 formation" step. This indicates that H_2 formation will occur spontaneously, sustained by H diffusion into the platelet from the surrounding H-supersaturated Si matrix. This mechanism is confirmed by a series of density functional theory (DFT) calculations [29] and supported by Raman spectroscopy, IR spectroscopy, and forward recoil scattering experiments [4,32].

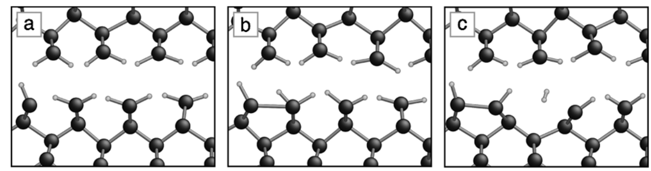

FIG. 2. Formation of H_2 during the dihydride-to-monohydride reconstruction of the HIP surfaces. An unsaturated Si-H group approaches an adjacent doubly hydrogenated Si atom (a), producing an intermediate H-Si-Si-2H structure (b). Later, one of the two H atoms bound to the overcoordinated Si atom desorbs and binds to a H atom of a neighboring Si-2H group, producing a stable H-Si-Si-H dimer, a free H_2 molecule, and a novel unsaturated Si-H group (c).

During further LOTF annealing simulations, some of the H_2 molecules reach the platelet edges. Here, we observe one of the strained Si-Si bonds [connecting the red atoms in Fig. 3(a)] to break, while a H_2 molecule diffuses close to the two Si atoms [blue in Figs. 3(a)–3(c)]. The molecule eventually dissociates [Fig. 3(d)], irreversibly saturating the newly formed Si dangling bonds. This is consistent with the barrierless H_2 dissociation observed in the proximity of strained Si-Si bonds of small H_2/Si defect systems [33]. DFT calculations on a 90 Si atom (sub)system modeling the edge region of the HIP at a time immediately preceding the Si-Si bond breaking yield a 1.2 eV net driving force for the breaking event [29]. Since the formation of the new hydrogenated surfaces is endothermic in a stress-free system (by 0.25 eV per surface Si atom in our DFT calculations on free surfaces), this enthalpic gain must be a consequence of the local relaxation of the elastic field in the platelet edge region.

In two further LOTF MD simulations on the platelet system, stemming from the previous one, we remove the H_2 molecule immediately before and just after the breaking of the Si-Si bond, in both cases well before H_2 dissociative chemisorption has a chance to occur. In these two cases, the maximum distance between the two Si atoms is 3.0 and 3.7 Å, respectively [Fig. 3(e)]. However, in both cases the bond reforms shortly afterwards, indicating that H_2 is necessary to make such breaking irreversible. Moreover, hydrogen seems to play an active role in promoting the Si-Si bond breaking of HIP edge atoms. For instance, the H atom depicted in green in Fig. 3(a) is observed to hop from a Si atom to a neighbor dangling bond [Fig. 3(b)] just before the Si-Si bond-breaking event [Fig. 3(c)]. However, if this atom is prevented from hopping by applying a fixed constraint on the Si-H bond distance, the approaching H_2 molecule is sterically hindered from reaching the strained Si-Si bond, and no bond breaking is observed [Fig. 3(e)].

These results reveal that platelet growth, ultimately driven by the H supersaturation of the Si crystal matrix,

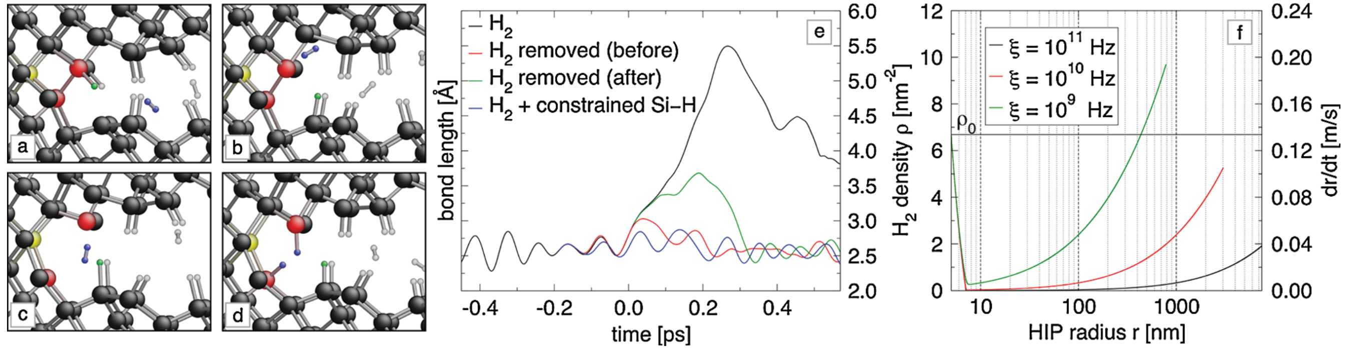

FIG. 3 (color). Stress-corrosion mechanism for the HIP's growth. (a)–(d) Snapshots of the bond-breaking reaction from an 800 K LOTF MD simulation (colors explained in the text). (e) Time evolution of the distance between the Si atoms pictured in red in (a)–(d) (black line). The time axis zero is set to the moment the bond length exceeds 2.8 Å just before bond breaking. The red and green lines refer to additional simulations, where the H_2 molecule [blue in (a)–(c)] is removed from the system 180 fs before and 20 fs after the bond-breaking event, respectively. The blue line represents the bond length evolution obtained if the H_2 molecule is not removed, but the transfer of the H atom colored in green in (a)–(b) is prevented. (f) Evolution of the density ρ of H_2 molecules formed inside the HIP, displayed as a function of the platelet radius r during platelet growth. The horizontal solid line indicates the initial value of the H_2 density ρ_0. The right-hand vertical axis coordinate is scaled so that the HIP radial velocity for $\xi = 10^9$ Hz, in $\mathrm{m\,s^{-1}}$ units, is represented by its corresponding curve.

can proceed without a H_2 internal pressure, through a series of stress-corrosive subcritical fracture propagation steps including (i) the spontaneous formation of H_2 molecules inside the HIP volume, (ii) the occasional breaking of strained Si-Si bonds at the platelet edges promoted by the arrangement and dynamical behavior of hydrogen atoms, and (iii) the dissociation of H_2 at broken Si-Si bonds making the platelet growth irreversible. Nevertheless, in the mesoscale models proposed to date [11–14], the HIP growth has been assumed to proceed via supercritical fracture propagation induced by the internal pressure exerted by H_2 molecules within the platelets, irrespective of their size. In this case, stress corrosion will still contribute to fracture propagation but may possibly not be the dominant propagation mechanism. We note, however, that H_2 dissociation at the HIP perimeter counteracts the formation of H_2 molecules on the platelet internal surfaces, and the relative rate of these two processes depends on the platelet size. It is therefore not obvious that any significant H_2 pressure buildup can actually occur in small platelets.

To investigate the balance between H_2 formation and dissociation and the possibility of H_2 pressure buildup effects, we model a HIP as a horizontal disk of radius r with constant vertical thickness. We consider a surface H_2 density ρ, representing the number of H_2 molecules inside the HIP per unit section area. This can be assumed to be spatially homogeneous at all times due to the high diffusivity of H_2 inside the platelet. In particular, the H_2 self-diffusion coefficient is a few orders of magnitude larger than the diffusion coefficient of H in crystalline Si [34]. If we define an "active" distance σ from the HIP edges within which H_2 molecules can spontaneously dissociate (typically taken to be the sum of the Si and H covalent radii), we find that, as r grows by successive stress-corrosive events, its time derivative can be expressed by $\dot{r} = (\xi\sigma\eta^{-1})\rho$ (derived in Ref. [29]). In this first-order reaction kinetics, the crack front propagation speed $\dot{r}$ is directly proportional to the H_2 reactant density ρ. The proportionality constant is given by the probability per unit time ξ for an active molecule to accomplish a stress-corrosion step, and by the geometric factors σ and η, the latter being the number of H_2 molecules required to saturate the newly formed monohydride (100) Si surfaces, per unit platelet area (6.68 molecules/nm^2 [29]).

The time variation of ρ can be modeled by $\dot{\rho} = k - 2(\xi\sigma r^{-1})\rho - 2(\xi\sigma r^{-1}\eta^{-1})\rho^2$ (see Ref. [29]), where the first right-hand term is the number of molecules forming in the platelet per unit of time and HIP area, the second term represent the loss of H_2 molecules due to dissociative chemisorption at the HIP's circular perimeter, and the third term accounts for the H_2 density decrease due to the platelet's area increase. The H_2 formation rate k is ultimately limited by H diffusion in the bulk Si matrix [3,5] and is estimated by a continuum diffusion model [29]. Using $D = 10^{-6}\ \mathrm{cm^2\,s^{-1}}$ as an upper bound estimate for the diffusion coefficient of H in crystalline Si at 800 K [35], we obtain $k \simeq 10^7\ \mathrm{nm^{-2}\,s^{-1}}$. Similarly, we estimate a lower bound $\xi_L = 5 \times 10^9$ Hz for the stress-corrosion event rate from density functional tight binding calculations on the 90 atom model already used above [29].

We solve the two coupled differential equations numerically, by using an initial HIP radius of 5 nm. This leads to the $\rho(r)$ dependence shown in Fig. 3(f) for three ξ values in the 10^9–10^{11} Hz interval. The initial H_2 density is arbitrarily set to $\rho_0 = 6.68\ \mathrm{nm^{-2}}$, corresponding to complete dihydride-to-monohydride reconstruction of fully saturated HIP surfaces. In all cases, the H_2 density decreases very rapidly during an initial transient stage, and a minimum is reached at a radius value close to 8 nm, after which ρ increases again with increasing slope. Crucially, even for

$\xi \simeq 10^9$ Hz, i.e., a fifth of our estimated lower bound, the initial ρ_0 value is recovered only for platelet radii larger than 435 nm. The same behavior is obtained irrespective of the initial density used, as any excess molecules initially present inside the platelet would readily dissociate and chemisorb at the platelet edges, due to the large perimeter to surface ratio in small HIPs. Even assuming a H_2 density as high as ρ_0, a simple calculation based on the ideal gas law would produce an estimated internal pressure lower than 200 MPa. According to linear elastic fracture mechanics [14], a 200 MPa internal pressure in a penny-shaped crack with 1 μm diameter yields a stress intensity factor $K_I = 0.16$ MPa$\sqrt{m}$, which is less than one-fifth of the Si fracture toughness [16]. This suggests that supercritical fracture could occur at the HIP edges only for H_2 densities much larger than ρ_0. However, for submicrometric HIPs this is ruled out by the kinetics of the stress-corrosion reaction.

Our results thus indicate that pressure-induced supercritical HIP growth does not take place for platelet diameters smaller than about 1 μm. HIPs are instead expected to grow via a subcritical stress-corrosion mechanism, powered by stress intensification at the platelet edges, with initial growth speeds of a few mm s^{-1} [Fig. 3(e)]. This is consistent with the remarkably slow platelet growth observed experimentally [5,6,36]. Moreover, a slow stress-corrosion growth is expected to produce a system of parallel platelets whose internal surfaces are entirely free from the ridgelike corrugated structures typically created in Si by high-speed propagation instabilities [18]. Indeed, careful atomic force microscope observations [8,15] reveal smooth cleavage surfaces after HIP growth and final sample failure, with rms roughness of the order of 1 nm.

In conclusion, our findings suggest that, while hydrogen implantation still ultimately provides the net thermodynamic driving force for cleavage, it is the kinetic aspects of HIP growth, with its specific coupling of chemical and elastic processes yielding slow accretion, which drive the formation of the remarkably smooth cleavage surfaces obtained in the experiments. While similarly slow initial HIP growth is expected in any host matrix where stress corrosion provides the main growth mechanism, these results have direct and straightforward implications on the fundamental limits of the Si ion-cut technique. For instance, there is a considerable gap between the $\sim 10^{-11}$ m s^{-1} initial HIP growth speed obtained in the experiments [6] and the $\sim 10^{-3}$ m s^{-1} upper bound for the same quantity estimated in this work. This indicates that limiting the diffusion of hydrogen feedstock into a growing platelet could provide a simple way to produce micrometer-sized atomically flat hydrogenated Si surfaces. At the opposite, technological extreme, any means of accelerating the transport of hydrogen to the platelets through the silicon matrix could, in principle, very significantly accelerate the cleavage process without compromising the smoothness of the final surfaces.

The authors are indebted to Stefan Estreicher, Gabor Csányi, James Kermode, and Lars Pastewka. We acknowledge funding from the EPSRC (EP/C523938/1), the DFG (CI144/2-1 and Gu367/30), and the EU-FP7-NMP Grant No. 229205 "ADGLASS." Computer time was allocated at KCL (London), HLRS (Stuttgart), SCC (Karlsruhe), and ZIH (Dresden).

*moras@iwm.fraunhofer.de

[1] E. Guyer and R. Dauskardt, Nature Mater. **3**, 53 (2004).
[2] G. Csányi *et al.*, Phys. Rev. Lett. **93**, 175503 (2004).
[3] B. Terreault, Phys. Status Solidi A **204**, 2129 (2007).
[4] M. Weldon *et al.*, J. Vac. Sci. Technol. B **15**, 1065 (1997).
[5] B. Aspar *et al.*, Microelectron. Eng. **36**, 233 (1997).
[6] J. Grisolia *et al.*, Appl. Phys. Lett. **76**, 852 (2000).
[7] T. Höchbauer *et al.*, J. Appl. Phys. **92**, 2335 (2002).
[8] B. Aspar *et al.*, J. Electron. Mater. **30**, 834 (2001).
[9] M. Bruel, Electron. Lett. **31**, 1201 (1995).
[10] S. Reboh *et al.*, J. Appl. Phys. **105**, 093528 (2009).
[11] L. B. Freund, Appl. Phys. Lett. **70**, 3519 (1997).
[12] C. M. Varma, Appl. Phys. Lett. **71**, 3519 (1997).
[13] W. Han and J. Yu, J. Appl. Phys. **89**, 6551 (2001).
[14] F. Yang, J. Appl. Phys. **94**, 1454 (2003).
[15] Y. J. Chabal *et al.*, Physica (Amsterdam) **273B–274B**, 152 (1999).
[16] G. Michot, Crystal Prop. Prep. **17–18**, 55 (1988).
[17] R. Pérez and P. Gumbsch, Phys. Rev. Lett. **84**, 5347 (2000).
[18] J. R. Kermode *et al.*, Nature (London) **455**, 1224 (2008).
[19] G. Moras *et al.*, Physica (Amsterdam) **401B–402B**, 16 (2007).
[20] T. Frauenheim *et al.*, Phys. Status Solidi B **217**, 41 (2000).
[21] F. H. Stillinger and T. A. Weber, Phys. Rev. B **31**, 5262 (1985).
[22] S. Frabboni, Phys. Rev. B **65**, 165436 (2002).
[23] Z. F. Di *et al.*, Appl. Phys. Lett. **93**, 104103 (2008).
[24] F. A. Reboredo, M. Ferconi, and S. T. Pantelides, Phys. Rev. Lett. **82**, 4870 (1999).
[25] N. Martsinovich, I. Suarez Martinez, and M. I. Heggie, Phys. Status Solidi C **2**, 1771 (2005).
[26] S. Romani and J. H. Evans, Nucl. Instrum. Methods Phys. Res., Sect. B **44**, 313 (1990).
[27] M. Nastasi *et al.*, Appl. Phys. Lett. **86**, 154102 (2005).
[28] J. G. Swadener, M. I. Baskes, and M. Nastisi, Phys. Rev. B **72**, 201202(R) (2005).
[29] See supplementary material at http://link.aps.org/supplemental/10.1103/PhysRevLett.105.075502 for details of the simulations and the mesoscale model.
[30] G. Moras *et al.*, in *Trends in Computational Nanomechanics*, edited by T. Dumitrica (Springer, Berlin, 2010).
[31] E. Romano *et al.*, Mater. Sci. Eng. B **159–160**, 173 (2009).
[32] Y. Ma *et al.*, Phys. Rev. B **71**, 045206 (2005).
[33] S. K. Estreicher, J. L. Hastings, and P. A. Fedders, Phys. Rev. B **57**, R12 663 (1998).
[34] S. H. Chen, T. A. Postol, and K. Sköld, Phys. Rev. A **16**, 2112 (1977).
[35] S. Bédard and L. J. Lewis, Phys. Rev. B **61**, 9895 (2000).
[36] L. J. Huang *et al.*, Appl. Phys. Lett. **74**, 982 (1999).